Review Article

Anthony Garetto, Thomas Scherübl* and Jan Hendrik Peters

Aerial imaging technology for photomask qualification: from a microscope to a metrology tool

Abstract: Photomasks carry the structured information of the chip designs printed with lithography scanners onto wafers. These structures, for the most modern technologies, are enlarged by a factor of 4 with respect to the final circuit design, and 20–60 of these photomasks are needed for the production of a single completed chip used, for example, in computers or cell phones. Lately, designs have been reported to be on the drawing board with close to 100 of these layers. Each of these photomasks will be reproduced onto the wafer several hundred times and typically 5000–50 000 wafers will be produced with each of them. Hence, the photomasks need to be absolutely defect-free to avoid any fatal electrical shortcut in the design or drastic performance degradation. One well-known method in the semiconductor industry is to analyze the aerial image of the photomask in a dedicated tool referred to as Aerial Imaging Measurement System, which emulates the behavior of the respective lithography scanner used for the imaging of the mask. High-end lithography scanners use light with a wavelength of 193 nm and high numerical apertures (NAs) of 1.35 utilizing a water film between the last lens and the resist to be illuminated (immersion scanners). Complex illumination shapes enable the imaging of structures well below the wavelength used. Future lithography scanners will work at a wavelength of 13.5 nm [extreme ultraviolet (EUV)] and require the optical system to work with mirrors in vacuum instead of the classical lenses used in current systems. The exact behavior of these systems is emulated by the Aerial Image Measurement System (AIMS™; a Trademark of Carl Zeiss). With these systems, any position of the photomask can be imaged under the same illumination condition used by the scanners, and hence, a prediction of the printing behavior of any structure can be derived. This system is used by mask manufacturers in their process flow to review critical defects or verify defect repair success. In this paper, we give a short introduction into the lithography roadmap driving the development cycles of the AIMS systems focusing primarily on the complexity of the structures to be reviewed. Second, we describe the basic principle of the AIMS technology and how it is used. The last section is dedicated to the development of the latest generation of the AIMS for EUV, which is cofinanced by several semiconductor companies in order to close a major gap in the mask manufacturing infrastructure and the challenges to be met.

Keywords: AIMS; defect review; EUV; lithography roadmap; mask metrology; SMO.

***Corresponding author: Thomas Scherübl,** Carl Zeiss SMS, Carl-Zeiss-Promenade 10, 07745 Jena, Germany, e-mail: scheruebl@smt.zeiss.com
Anthony Garetto and Jan Hendrik Peters: Carl Zeiss SMS, Carl-Zeiss-Promenade 10, 07745 Jena, Germany

1 Introduction

The semiconductor industry is a consensus-driven industry regarding the technologies used, when they are required and what specifications need to be met. This long-term forecast, over a period of 10–15 years, is reviewed every year with a major release cycles of 2 years – the so-called ITRS roadmap [1]. A major element in this roadmap are technology decision points about when a certain technology will have to be production ready and which technical specifications need to be fulfilled by that date. It also displays the current readiness of the industry marked by a color code [manufacturable solutions are known (yellow)/not known (red)] as seen in Figure 1.

Defects are an inherent part of the manufacturing process for high-end photomasks. Sources of defects vary from particle inclusions in the resist or cleaning liquids, debris coming from the process chamber, or embedded defects in the base material – the mask blank. Any defect that is larger in size than about one fourth of the smallest open structure could potentially destroy the performance

Year of production	2011	2012	2013	2014	2015	2016	2017	2018
DRAM 1/2 pitch [nm]	36	32	28	25	23	20	18	16
DRAM /Flash CD control (3 sigma) [nm]	3,7	3,3	2,9	2,6	2,3	2,1	1,9	1,7
Substrate defect size [nm]	37	35	34	32	30	29	27	26
Blank defect size [nm]	29	25	23	20	18	16	14	13

Figure 1 Extraction of the ITRS Roadmap 2011 of the structure sizes on EUV photomasks for a given technology node (e.g., given as DRAM half pitch size in [nm]) and the required defect size to be identified, repaired, and reviewed for repair success.

of the chip and therefore has to be corrected. Figure 2 shows an example of such a defect on an extreme ultraviolet (EUV) mask, which must be found and repaired as well as the effect the defect has when the mask is printed on an EUV scanner [2, 3]. Defects for the 193-nm photomasks are usually an excess or lack of absorber material. For EUV masks, in addition to these surface shape deviations (also called absorber defects) are defects embedded in the mirror multilayer material (multilayer defects). Any particle of the same size in the open areas would have a similar effect. These particles could, for instance, be created or deposited by transportation or handling of the mask.

For the 193-nm photomasks, the pattern can be very complicated to compensate for subresolution image artifacts, which are already accounted for in the mask design. The mask pattern design is enhanced by nonprinting structures, so-called OPC features (optical proximity correction), which are needed to obtain the resolution of the intended structures. For even more complex patterns, the mask layout and the illumination aperture of the scanner (source) are optimized simultaneously [source mask optimization (SMO)]. As a result, complex scanner illuminators (SMO illumination), together with complex mask designs, are needed to print a certain pattern on the wafer. Figure 3 shows from left to right the illuminator optimized for the mask pattern needed to create the desired structure on the wafer. The last two pictures show that the aerial image as seen by the AIMS tool is identical to the wafer image in resist.

As photomasks have to be defect-free, repair is a standard process step in mask fabrication. Mask repair is performed, for example, using the e-beam-based mask repair tool MeRiT® [4]. In the MeRiT®, an electron beam column is combined with a gas injection system. Depending on the gases used, the e-beam triggers a chemical reaction, and the material can be either etched or deposited on the nanometer scale.

The criterion for a successful repair is that the defect will not print on the wafer. In principle, this can be verified by doing a test wafer print using the repaired mask and comparing the wafer print of the repaired feature to a nonrepaired feature. In real life, such a procedure has severe limitations, both economically and practically. Mask shops are operated separately from wafer fabs and have no access to scanners and a complete wafer processing line. This infrastructure requires high investments, which cannot be justified for mask repair verification only. This motivation led to the development of the AIMS system by the early 1990s [5].

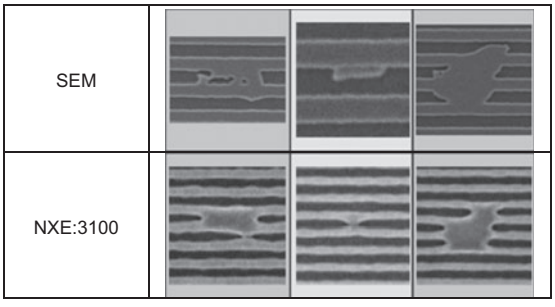

Figure 2 Example of defects in an EUV photomask pattern for the 32-nm node. Images are from Ref. [2]. The top row shows the defects as imaged by an SEM on the photomask; the bottom row shows the image of the photomask defect as printed in resist with an NXE:3100 EUV scanner.

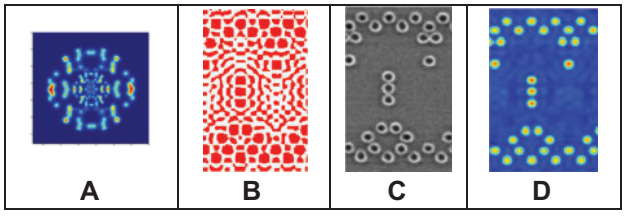

Figure 3 SMO illumination of a contact hole structure. From left to right (A) the illuminator optimized for (B) the mask pattern needed to create (C) the desired structure printed on the wafer. (D) The aerial image as seen by the AIMS tool.

2 Principle of AIMS: from a microscope to a metrology tool

2.1 Basic AIMS setup

The fundamental idea behind the AIMS system is to emulate the scanner imaging on the wafer by a special microscope. Figure 4 shows a schematic comparison of a scanner to an AIMS system. A scanner illuminates the mask using a certain wavelength and illumination aperture. In state-of-the-art scanners, the image field is defined by a slit with a typical size of 150 mm×10 mm. The mask is scanned along the slit, and all light diffracted by the mask features is collected by the NA of the objective lens. The scanner lens demagnifies and images the mask features on the wafer. The large image field of 150 mm×10 mm, combined with a high NA of 1.35, leads to large and very complex scanner imaging lenses. The AIMS system, on the contrary, has a small field of view, typically 10 µm×10 µm at mask level. This small field is just big enough to capture the whole defect or repaired defect on the mask.

The location of a defect is detected by a mask inspection system. These systems scan the entire mask with high-resolution optics to locate defects. As an output, a defect coordinate list is created where the location of a defect is known with an accuracy of 1 µm. This coordinate list is used as input for the AIMS system, which moves automatically to the location of the defect. The defect is illuminated by the AIMS (Figure 4) with the same wavelength and illumination apertures the scanner uses. The imaging lens of the AIMS has the same NA on the mask side as the scanner. Consequently, in the AIMS, the light, which is diffracted by the mask, is collected in exactly the same way as on the scanner. The difference is that in the case of the AIMS, the image is magnified by the imaging lens on a CCD camera and not reduced to the wafer as in the scanner. All essential parameters that determine the aerial image, such as wavelength, illumination type, and NA of the imaging lens, are identical to the scanner. All optical effects leading to the formation of the aerial image, including diffraction, the optical properties of the mask material, and the collection by the NA of the scanner, are detected by the CCD camera of the AIMS in the same way as on the scanner. The CCD camera of the AIMS sees the aerial image just as the wafer sees it. Thus, by comparing the aerial image of a defect or a repair to a nondefective and nonrepaired location of the same features on the mask, the success of a repair can be verified [6–9]. The advantage is that no scanner and no wafer prints are necessary. This process flow is also shown in Figure 5.

During the wafer processing, the resist properties and behavior also contribute to the final wafer printing. These resist effects are naturally not captured by the AIMS image. However, several studies have been performed showing that the AIMS measurements have an excellent correlation to the wafer prints and predict the wafer printing results accurately (see, for example, [10, 11]). By combining the AIMS aerial image with a subsequent resist simulation, the correlation to the wafer prints can further be improved [12, 13]. With the introduction of the immersion scanners, the so-called vector effects and polarization effects became more dominant in scanner printing. Consequently, these generations of AIMS tools have been equipped with polarizers. Additionally, a special measurement mode for the AIMS, the so-called “scanner mode”, has been introduced to the AIMS tools. The use of the scanner mode allows emulation of the aerial image in the resist taking the vector effects into account. A detailed

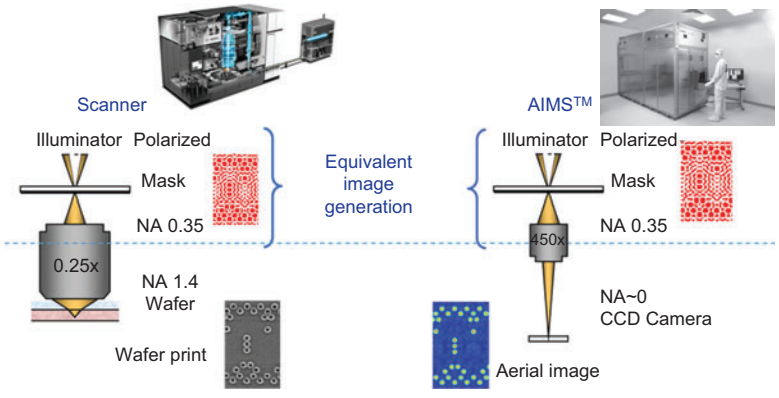

Figure 4 Schematic comparison of the optical setup of a scanner (left) to an AIMS system (right).

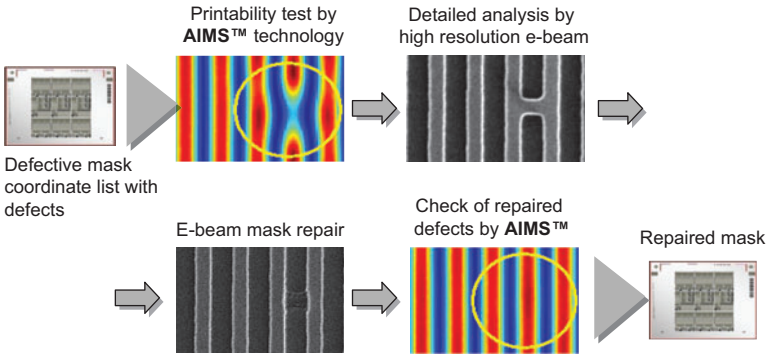

Figure 5 AIMS™ measurements in the mask repair process.

description and analyses of the scanner mode can be found in [11].

Optical lithography has always been driven by shrinking the feature sizes. In the scanner development, this has led to scanners with smaller wavelengths going from 365 nm to 248 nm to 193 nm, increasing NAs, and the introduction of immersion lithography as well as SMO techniques. The next step is the introduction of EUV lithography. The AIMS technology and tool development must always be synchronized with the scanner roadmap. This leads to an evolution of the AIMS systems [14–18] from a modified manually operated microscope in 1994 to a fully automatic metrology tool as shown in Figure 6. The first AIMS system was introduced into the market under the brand name microlithography simulation microscope (MSM) in 1994. It was based on a modified DUV microscope working with 248 nm. The operation was purely manual, and the operator had access to the back aperture plane where the different illumination apertures were inserted manually. With advanced lithography nodes, the AIMS technology became a standard technology in photomask fabrication. The AIMS™ fab system introduced in 2000 was the first automated AIMS system designed for use in a production environment. Although from the basic idea the AIMS™ is a microscope setup, the AIMS systems have totally different requirements, which must be considered in the design.

First, the optical performance of an AIMS must be similar to a scanner. Second, the AIMS verifies if a repair on the mask was successful or not by measuring the relative change in the critical dimension (CD) of the aerial image [19, 20]. The CD measured at a given threshold of the aerial image of the repaired defect is compared to a nondefective and nonrepaired reference feature (see Figure 7). Therefore, aside from the optical parameters, the CD repeatability has become an important parameter of current AIMS generations. Tool stability as well as long-term repeatability has become more and more important. Since the market introduction of the first AIMS in 1994, the AIMS technology has evolved from a "special" microscope to a highly sophisticated metrology tool as represented by the latest AIMS generation, the AIMS™ 32-193i. In the next paragraphs, the main requirements and challenges for an AIMS system are discussed using the latest AIMS generation.

Figure 6 Evolution of the AIMS technology over 16 years.

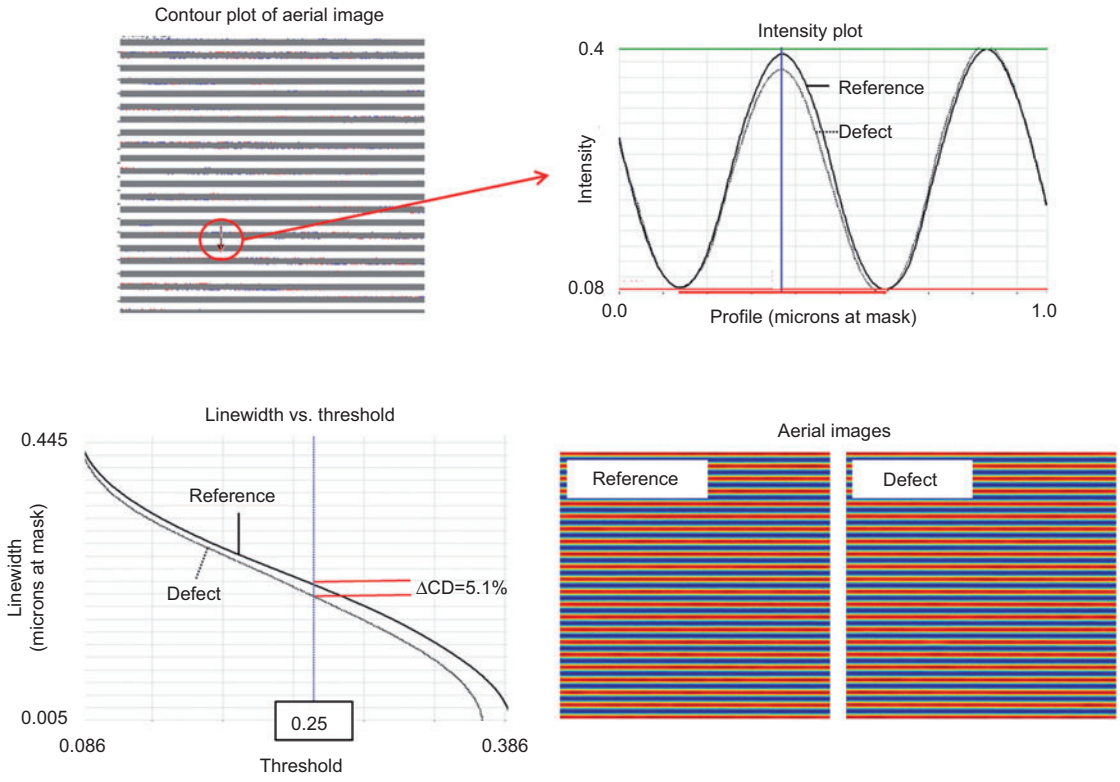

Figure 7 A typical AIMS™ analysis. The aerial images of the defect and the reference feature are shown in the lower right. Visually, a difference is hard to see. In the AIMS™ analysis, both images are overlaid (upper left), the intensity profiles are plotted (upper right, dotted line: defect), and the difference in the CD at a function of the aerial image intensity is calculated (lower left). In this example, the CD difference is 5.1% relative to the reference at a normalized aerial image intensity of 0.25.

2.2 General system overview

A schematic overview of the AIMS™ 32-193i is shown in Figure 8. The system consists of a precise interferometer-controlled stage carrying the mask to move the defect into the center of the field of view. An excimer laser is used as the light source. The illumination unit consists of a beam homogenizer, an illumination system, and a condenser lens. The objective lens, together with post-magnifying optics, generates the aerial image on the CCD camera. In order to maintain stable measurement conditions ensuring long-term CD stability and repeatability, the whole optical system is kept under constant temperature by an environmental control system. Additionally, the system is acoustically isolated, and the mask is kept under constant airflow ensuring that no particle contamination occurs.

2.3 AIMS illumination unit

The coherent laser beam generating a 193-nm light requires a special homogenizer, which has been developed for AIMS. As the AIMS magnifies the image on a CCD camera, the etendue is extremely small. This is a significant difference to optical scanners, which have a large etendue due to the large fields (mm range compared to 10 µm in the AIMS). Technologies for beam homogenization used in scanners, therefore, cannot be applied to AIMS systems, and special beam homogenization technologies had to be developed for the small etendue of the AIMS systems.

After the homogenizer unit, the beam enters the illumination system where the illumination aperture can be changed according to the user requirements. The illumination shapes used in state-of-the-art scanners vary from classical configurations like on-axis illumination, dipole, disar, etc. to more sophisticated SMO illumination types with variable shapes and transmissions (Figure 9). About 100–200 classical illuminators can be selected by the user. The selection runs fully automatic and is adapted to the specific requirements of the customer. The user can define a dedicated measurement recipe, which then automatically selects the required aperture. The SMO-type illuminator can be generated in the AIMS™ 32-193i by using a special device called “free form illumination”. These

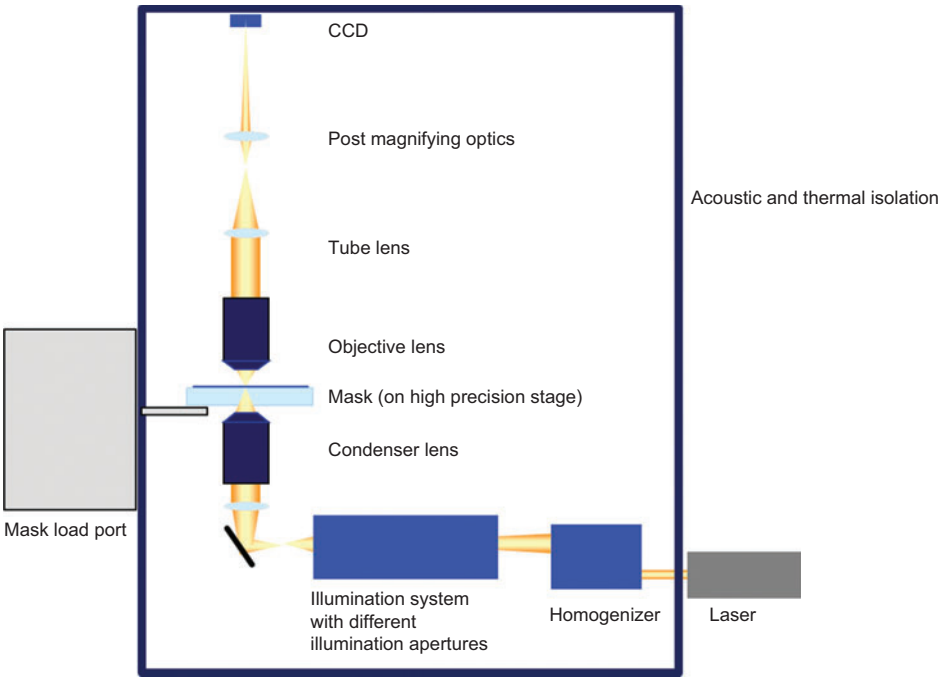

Figure 8 The AIMS™ 32-193i principal setup.

devices are fabricated according to the user requirements and generate a specific illumination shape where also the transmission in the aperture can be varied. For each SMO type, a specific "free form device" has to be manufactured.

With the introduction of the 193-nm immersion, the use of polarized illumination has also been introduced into scanners. The AIMS™ 32-193i is equipped with polarizers, which enable the use of tangential or linear polarized light for illumination identical to those in a scanner [21].

2.4 Imaging optics

The NA of the imaging optics has to be equivalent to that used in the scanner. For the current immersion scanners, the highest supported NA is 1.35 at wafer; this corresponds to an NA of 0.3375 at the mask level for the objective lens. One main difference from the scanner is the magnification on a CCD camera and the small field of view of the AIMS. Scanner lenses are large in diameter as they have to support a large field of view and a high NA. The AIMS, instead, has a very small field of view. Therefore, the lens diameters are small, and the size is similar to the objective lenses in microscopy. The image quality of an AIMS has to be similar to a scanner. This requires the development of special lens mounting and manufacturing technologies specifically for small lens diameters used in the AIMS. The AIMS™ 32-193i uses the newly developed LITO™ grade optics, which gives the highest imaging performance.

3 AIMS™ EUV: next generation design

To overcome the resolution limit of 193 nm, the industry has decided to use 13.5 nm (EUV) as the new wavelength

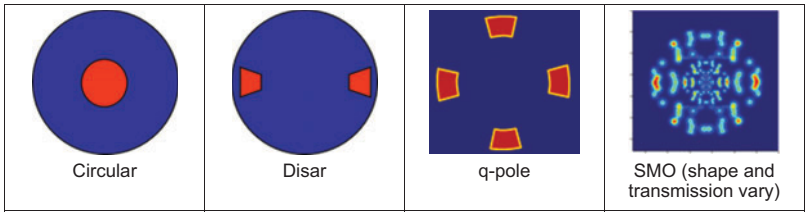

Figure 9 Examples of different illumination apertures supported by the AIMS™ 32-193i.

for lithography. This switch to EUV technology, more than with any other previous transition, requires a change in the industry's infrastructure [22]. What makes this transition particularly challenging, in addition to the need for a new illumination source, is that no materials are optically transparent at 13.5 nm. Therefore, the refractive optics of previous generations must be replaced with reflective optics, and the entire metrology process must occur under vacuum.

Because the application of the AIMS system requires the metrology of the photomask features under scanner-like conditions, the design of an AIMS™ EUV system approaches that of an EUV scanner in complexity [23, 24]. The 13.5-nm wavelength photons can no longer be produced by a laser alone and require a discharge-produced plasma (DPP) or laser-produced plasma (LPP) that utilizes Sn, Xe, or Li as a source. The source power is a major challenge for scanner systems that require a specific dose to clear photoresist and maintain a throughput consistent with high-volume manufacture (HVM). Another concern is debris created by the source, which degrades components and causes an increase in the cost of ownership as these components must frequently be replaced. While debris creation is also a concern with the AIMS™ EUV, the source power is not an issue as the only requirement is to produce an aerial image of a very small surface segment of the photomask features. On the other hand, source brightness (source power in a small light cone) needs to be high enough for high measurement throughput and accuracy.

To achieve a high reflectivity of the optics at 13.5 nm, a multilayer (ML) mirror system utilizing Bragg reflection to produce constructive interference is employed for each mirror. The basic design for an EUV ML mirror consists of alternating layers of Si and Mo. The uppermost layer is coated with a protective capping layer. The structural design including the bilayer thickness and γ ratio must be optimized in order to ensure maximum reflectivity at the desired wavelength. Over 40 bilayer pairs are required to reach reflectivity values close to the theoretical limit of 70%. The most advanced optics processes to date are required in order to achieve suitable surface figure quality with mid spatial frequency range (MSFR) values below 0.10 nm (Figure 10).

Figure 11 shows the design of the optical path for the AIMS™ EUV. The photons are produced at the source and collected by the first mirror at the collector module (IL1) after which they pass through the intermediate focus module. The illumination is defined by the sigma before hitting mirrors 2 (IL2) and 3 (IL3) after which the radiation is focused onto the photomask (not shown), and the illumination of the mask is completed. After the reflection of the photomask, the NA is defined, and the light continues along the optical path of the remaining three mirrors (M1–M3), which focus the image onto a CCD for imaging.

Another complexity of the AIMS™ EUV over previous generations is the prerequisite for the entire system to be held under vacuum so that the EUV photons can traverse the entire optical path without being absorbed by molecules present in an atmospheric environment. Additionally, EUV photons interacting with ML surfaces induce secondary electrons (SE) which in turn interact with water or hydrocarbon (HC) molecules adsorbed to the mirror surface. These SEs provide the energy required to break the molecular bonds and result in the formation of oxides or carbon contamination on the surface. An increase in the natural oxide layer thickness or accumulation of carbon deposition leads to an unacceptable loss in reflectance. A vacuum environment is therefore required both to allow EUV photons to traverse the optical path as well as to prevent the accumulation of contamination on

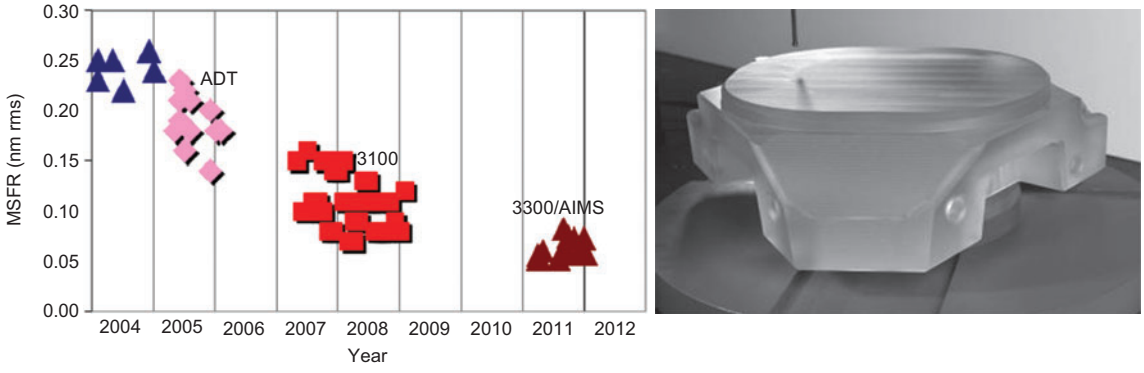

Figure 10 A graph showing the trend of obtainable MSFR for EUV optics for tool generations over time. The AIMS™ EUV utilizes the most advanced processes to reach the current scanner quality. The image on the right displays the rough shape of three of the AIMS™ EUV mirrors.

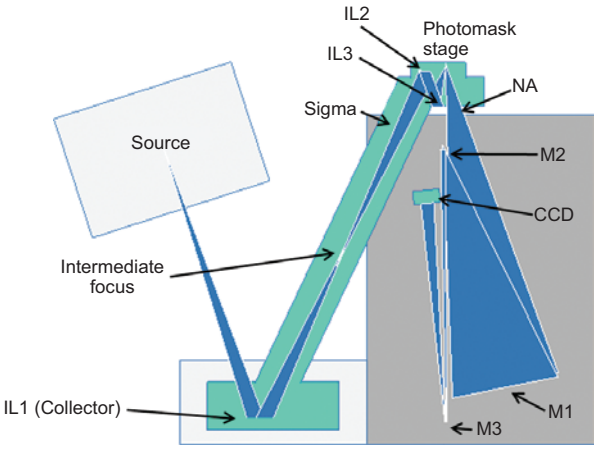

Figure 11 Sketch of the optical path design for the AIMS™ EUV consisting of a total of six mirrors, three at the illuminator side and three at the magnification side.

the surface of the reflective optics, which leads to a reflectance loss.

4 AIMS™ EUV application: EUV photomasks and defects

The EUV mask is a ML mirror on a substrate conceptually similar to those comprising the optical system but with an extra absorber layer deposited on the surface (Figure 12). The absorber layer is patterned and removed in specific areas according to a design in order to generate the desired aerial image under specific illumination settings that will be imaged on the photoresist.

The increased complexity of the EUV photomask has given rise to several new defect types. Both refractive masks and EUV masks are susceptible to absorber defects, which are flaws or damage to the patterned absorber layer. These defects can be clear defects where the absorber material is missing or opaque defects in the form of excess absorber material remaining in unwanted areas. The EUV masks alone have a new class of ML defects, which arise during the ML deposition process or are present on the substrate itself before the ML deposition [25]. The ML defects mostly originate from the boundary of the substrate surface and the ML. They can be generally classified as bump or pit defects and act as small lenses, themselves, with their own focusing properties, which lead to a reduced local intensity of the aerial image at the defect and the effect of one defocus direction becoming sharper. Bump defects cause a distortion in the wave front that diverges slightly toward the projection lens and is therefore sharper at a negative defocus position [26] (when the focal plane is above the reflective surface) and nearly disappears at a positive defocus position. Pit defects on the other hand produce a slightly converging wave front and become sharper at positive defocus positions (when the focal plane is below the reflective surface).

While the 193-nm AIMS tools have been used for several years in production, the AIMS™ EUV tool is still under construction [27–29]. The final design of the tool has been completed, and the assembly of the first prototype is on its way. Owing to the importance of this tool in the manufacturing flow, the development program is prefinanced by the EUV Mask Infrastructure Consortium, a collaboration of leading semiconductor manufacturing companies. The prototype will be ready for measurements in August 2014, and the commercial tools will follow shortly after.

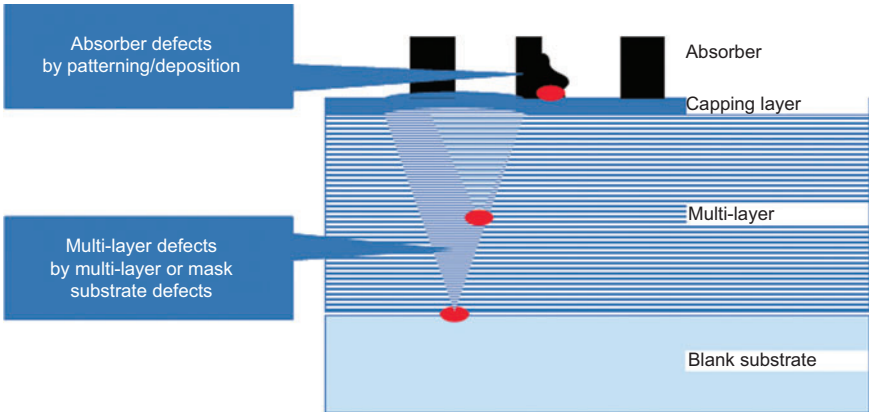

Figure 12 Cross-section diagram of an EUV photomask depicting the two major classifications of the absorber defects and ML defects. The ML defects consist of blank substrate defects propagating through the ML as well as those defects induced during the ML deposition process.

5 Summary

The concept of emulating a scanner, first introduced in 1994, by measuring the aerial image has become a de facto industry standard in mask making industry. The AIMS technology has been expanded over the years to always emulate the latest upcoming scanner generations. The AIMS tools are metrology tools working with a high degree of automation in the mask shop. The development of the next AIMS generation, the AIMS™ EUV has started to enable photomask making for EUV lithography.

Received June 11, 2012; accepted August 9, 2012

References

[1] ITRS roadmap (http://www.itrs.net/Links/2011ITRS/Home2011.htm). Accessed on 30 May 2012.
[2] T. Bret, M. Waiblinger, R. Jonckheere, D. Van den Heuvel and G. Baralia, Proc. of SPIE 8322, in press.
[3] R. Jonckheere, T. Bret, D. Van den Heuvel, J. Magana, W. Gao, et al., Proc. of SPIE 8166, 8166-3.
[4] A. Garetto, J. Oster, M. Waiblinger and K. Edinger, Proc. of SPIE 7488, 7844-15 (2009).
[5] R. A. Budd, D. B. Dove, J. L. Staples, R. M. Martino, R. A. Ferguson, et al., IBM J. Res. Dev. 41, 119–129 (1997).
[6] J. H. Peters, S. Perlitz, U. Matejka, W. Harnisch, D. Hellweg, et al., in 2011 International Symposium on Extreme Ultraviolet Lithography (2011).
[7] M. Waiblinger, et al., Proc. of SPIE (2011).
[8] A. Erdmann, P. Evanschitzky and T. Bret, Proc. of SPIE 8322, 8322-13 (2012).
[9] S. Perlitz, W. Harnisch, U. Strößner, H. Feldmann, D. Hellweg, et al., in 27th European Mask and Lithography Conference Proc. of SPIE 7985, 7985-29 (2011).
[10] E. van Setten, O. Wismans, K. Grim, J. Finders, M. Dusa, et al., Proc. of SPIE 6924, 6924-174 (2008).
[11] P. De Bisschop, V. Philipsen, R. Birkner, U. Buttgereit, R. Richter, et al., 67301, 67301G (2007).
[12] U. Strößner, H. Seitz, R. Birkner, R. Richter and T. Scherübl, Proc. of SPIE 7122, 7122-48 (2008).
[13] B. Meliorisz, A. Erdmann, T. Schnattinger, U. Strößner, T. Scherübl, et al., Proc. of SPIE 7028, 7028-95 (2008).
[14] A. Zibold, R. Schmid, K. Böhm, R. Brunner and A. Dürr, Proc. of SPIE 5835, 5835-115 (2005).
[15] A. Zibold, E. Poortinga, H. V. Doornmalen, R. Schmid, T. Scherübl, et al., in '21st European Mask and Lithography Conference', Proc. of SPIE 5853, 371–379 (2005).
[16] A. Zibold, R. Schmid, A. Seyfarth, M. Wächter, W. Harnisch, et al., Proc. of SPIE 5752, 1042–1049 (2005).
[17] J.-P. Urbach, K. Eisner, C. M. Schilz, T. Yasui, I. Higashikawa, et al., Proc. of SPIE 4889, 469–477 (2002).
[18] A. Zibold, N. Rosenkranz, U. Strössner, W. Harnisch and A. Williams, Proc. of SPIE 6283 (2006).
[19] A. Zibold, K. Böhm and A. Dürr, Proc. of SPIE 6152 (2006).
[20] A. Zibold, W. Degel, U. Stroessner, T. Scherübl, W. Harnisch, et al., Proc. of SPIE 6152 61522M-1 (2006).
[21] U. Strössner, E. Poortinga, W. Degel, T. Scherübl, N. Rosenkranz, et al., Proc. of SPIE 6281 628108-1 (2006).
[22] B. Rice, in 2009 International Symposium on Extreme Ultraviolet Lithography 2009).
[23] U. Stroessner, H. Feldmann, W. Harnisch, D. Hellweg and S. Perlitz, in 'AIMS™ EUV – Status of Concept and Feasibility Study', 2010 International Symposium on Extreme Ultraviolet Lithography (2010).
[24] H. Feldmann, J. Ruoff, W. Harnisch and W. Kaiser, Proc. of SPIE 7636, 76361C (2010).
[25] J. H. Peters, in 'EUV Defect Review and Repair', 8th Annual Mask Cleaning Workshop (2011).
[26] J. H. Peters and M. Waiblinger, in 'Enabling the EUV Infrastructure', SEMICON Korea 2012, S1. (Advanced Lithography, Seoul, Korea, 2012).
[27] D. Hellweg, J. Ruoff, A. Herkommer, J. Stühler, T. Ihl, et al., Proc. of SPIE 7969, 79690H (2011).
[28] S. Perlitz, W. Harnisch, U. Strößner, J. H. Peters, M. Weiss, et al., Proc. of SPIE 8166, 816610 (2011).
[29] D. Hellweg, S. Perlitz, M. Weiss, J. H. Peters, W. Harnisch und M. Goldstein, in 'SPIE Advanced Lithography, Extreme Ultraviolet (EUV) Lithography III', (2012).

Anthony Garetto received his BS in Physics from the Applachian State University and his Masters from North Carolina State University in Materials Science and Engineering. Since his employment with Carl Zeiss in 2006 he has held the positions of Applications Specialist and Applications Supervisor. Currently he is the Product Manager for AIMS EUV.

Thomas Scherübl received a diploma in Physics from the University of Heidelberg, Germany and a PhD in Materials Science from the Technical University of Berlin. He joined Carl Zeiss in 1996. Since then he has held various positions as project manager and R&D manager for inspection and metrology systems for the semiconductor industry. Currently, he is the Director of Product Management and Application at Carl Zeiss Semiconductor Metrology Systems (Carl Zeiss SMS).

Jan Hendrik Peters studied physics at the University of Hamburg, Germany, and University of Washington, Seattle. He received his PhD in particle physics in 1990. Until 2003 he worked at the Deutsches Elektronen-Synchrotron DESY research center in Hamburg. After receiving an MBA from the Nordakademie in Elmshorn in 2003, he moved to Dresden to work as R&D manager for future mask development at the Advanced Mask Technology Center, Dresden, including 157 nm, 193 immersion lithography and double patterning, as well as EUV technologies. He has led several national and international funded projects in these fields. Since 2010 he coordinates the mask related EUV activities of Carl Zeiss SMS and currently holds the position of the Director New Business Development.